



Photo-Fenton and Slow Sand Filtration coupling for hydroponics water reuse

M^a del Mar Micó Reche

ADVERTIMENT. La consulta d'aquesta tesi queda condicionada a l'acceptació de les següents condicions d'ús: La difusió d'aquesta tesi per mitjà del servei TDX (www.tdx.cat) i a través del Dipòsit Digital de la UB (diposit.ub.edu) ha estat autoritzada pels titulars dels drets de propietat intel·lectual únicament per a usos privats emmarcats en activitats d'investigació i docència. No s'autoritza la seva reproducció amb finalitats de lucre ni la seva difusió i posada a disposició des d'un lloc aliè al servei TDX ni al Dipòsit Digital de la UB. No s'autoritza la presentació del seu contingut en una finestra o marc aliè a TDX o al Dipòsit Digital de la UB (framing). Aquesta reserva de drets afecta tant al resum de presentació de la tesi com als seus continguts. En la utilització o cita de parts de la tesi és obligat indicar el nom de la persona autora.

ADVERTENCIA. La consulta de esta tesis queda condicionada a la aceptación de las siguientes condiciones de uso: La difusión de esta tesis por medio del servicio TDR (www.tdx.cat) y a través del Repositorio Digital de la UB (diposit.ub.edu) ha sido autorizada por los titulares de los derechos de propiedad intelectual únicamente para usos privados enmarcados en actividades de investigación y docencia. No se autoriza su reproducción con finalidades de lucro ni su difusión y puesta a disposición desde un sitio ajeno al servicio TDR o al Repositorio Digital de la UB. No se autoriza la presentación de su contenido en una ventana o marco ajeno a TDR o al Repositorio Digital de la UB (framing). Esta reserva de derechos afecta tanto al resumen de presentación de la tesis como a sus contenidos. En la utilización o cita de partes de la tesis es obligado indicar el nombre de la persona autora.

WARNING. On having consulted this thesis you're accepting the following use conditions: Spreading this thesis by the TDX (www.tdx.cat) service and by the UB Digital Repository (diposit.ub.edu) has been authorized by the titular of the intellectual property rights only for private uses placed in investigation and teaching activities. Reproduction with lucrative aims is not authorized nor its spreading and availability from a site foreign to the TDX service or to the UB Digital Repository. Introducing its content in a window or frame foreign to the TDX service or to the UB Digital Repository is not authorized (framing). Those rights affect to the presentation summary of the thesis as well as to its contents. In the using or citation of parts of the thesis it's obliged to indicate the name of the author.

Programa de doctorat: Ciència i Tecnologia de Materials

Memòria de tesis doctoral:

**PHOTO-FENTON AND SLOW SAND FILTRATION COUPLING FOR
HYDROPONICS WATER REUSE**

M^a del Mar Micó Reche

Dirigida per: Dra. Carme Sans Mazón. Professora titular del departament
d'Enginyeria Química de la Universitat de Barcelona.

Universitat de Barcelona

4

RESULTS AND DISCUSSION

The work which this thesis is based on was planned as the study of different aspects regarding the suitability of water reuse strategy in hydroponic greenhouses described in the introduction. As the different points of view of the integrated process between photo-Fenton reaction and Slow Sand Filtration Column were considered, the behavior of three structurally different pesticides was also monitored: methomyl, a carbamate insecticide; imidacloprid, a neonicotinoid insecticide; and fosetyl-Al, an organophosphorous fungicide.

The whole work of this thesis could be broken down in three stages. The first one is related to the analysis of photo-Fenton reaction over increasingly complex matrices. The efficiency of the oxidation was evaluated regarding to its capacity for depolluting artificial effluents starting from solutions just composed by water and the target pesticide. The concentration of the pesticide was monitored, together with the elimination of dissolved organic carbon, the evolution of biodegradability (in the shape of BOD₅/COD ratio) and in some cases also the progression of toxicity. Step by step the effluent submitted to photo-Fenton reaction was getting more and more complex by the addition of more than one target species at a time, and the supplement of inorganic salts. Other involved substances such as Fe or H₂O₂ concentrations were also monitored from that moment on. Increase the complexity of the problem solutions was carried out in order to test the robustness of the process against high conductivities; that is to say, to check the feasibility of applying this oxidation pretreatment to effluents coming from the recycling of the hydroponics system or even from the brine of the membrane separation stage proposed in the second strategy. The applicability of photo-Fenton reaction was also tested using solar light as source of radiation, as a promise of an easy and inexpensive place in field implementation of this Advanced Oxidation Process.

The second stage encompasses all the work related to the study of the biocompatibility of those increasingly complex effluents. Biodegradability and adaptation capability of microbial consortia was tested by Sequenced Batch Reactors at different points of the photo-Fenton performance study. The first one tried to find the biocompatibility shift for different intensity photo-Fenton reactions, regarding to different initial concentration

of reagents. The second one studied the biocompatibility of more complex, salt containing, and oxidized effluents. Not just from the point of view of the efficiency of the AOP, but also from the point of view of the different degrees of salinity that characterize those effluents. Those two biocompatibility essays gave a glimpse of the plausibility of photo-Fenton/bioreactor integration. Therefore the performance of a Slow Sand Filtration Column fed with pre-oxidized loads was essayed. This study showed how the integration is a sensible option even for salinities reaching $12 \text{ mS}\cdot\text{cm}^{-1}$.

The last stage includes all the work related to molecular biology tools. These novel techniques allowed to characterize the bacterial population developed in mentioned sequencing batch bioreactors and in the schmutzdecke layer of the slow sand filtration column.

This recapitulation of important results and conclusions from the papers and other publications, included as appendixes, pretends to summarize and highlight the most important milestones of the research this thesis is based on.

4.1. PHOTO-FENTON REACTION

COMPARISON BETWEEN OZONATION AND PHOTO-FENTON PROCESSES FOR PESTICIDE METHOMYL REMOVAL IN ADVANCED GREENHOUSES

Appendix I, (Micó et al. 2010b) introduces a starting study of comparison between photo-Fenton reaction and ozonation process over methomyl highly concentrated effluents.

It corresponds to the first steps of the research, when the experiments were focused in simple matrices containing just pure water and the commercial formulation of methomyl. Although in the last phases of the research the studies were focused in lower pesticide concentration, the researching process started with high concentration of the phytosanitary ($200 \text{ mg}\cdot\text{L}^{-1}$), just like it is recommended for traditional irrigation purposes (lower concentrations are recommended for hydroponics irrigation). This study pretended to point out their efficiency in degrading the pesticide content and mineralizing. Biodegradability and toxicity of the effluents were also important parameters to take into account.

Based on previous experiments, the best condition regarding to mineralization rate, photo-Fenton reaction was carried out with $300 \text{ mg}\cdot\text{L}^{-1}$ of hydrogen peroxide and $70 \text{ mg}\cdot\text{L}^{-1}$ of Fe(II) ¹. On the ozonation case, an average inlet ozone concentration of $10.5 \text{ mg}\cdot\text{L}^{-1}$ was used along the treatment, and the pH, initially around 4.5, evolved freely tending to 4.00.

¹ These reagent concentrations were very high compared to the ones used in the rest of the research. They are justified by the high initial concentration of pesticide and the fact that the research was at its very first steps.

Methomyl was not as effectively degraded by photo-Fenton reaction as by ozonation, but its mineralization was almost doubled by the photo-oxidative technique. Besides toxicity analysis, depicted in fig. 41, showed how from the very beginning of ozonation process toxic intermediates were being generated, as TU values increased during the first half hour and stayed high until the total depletion of the pesticide ($TU_0=5$, $TU_f=70$). In opposition to it, although photo-Fenton reaction caused oscillation on toxicity value, it tended to finally decrease at the reaction ($TU_0=5$, $TU_f=9$). The formulation of the product, with $200 \text{ mg}\cdot\text{L}^{-1}$ of ethanol, suggested the presence of an important biodegradable fraction in the solution. However, initial BOD_5/COD is quite low, 0.02 approximately (for $300 \text{ mg}\cdot\text{L}^{-1}$), and only reaches from 0.03 to 0.05 after photo-Fenton reaction and gets worse after ozonation.

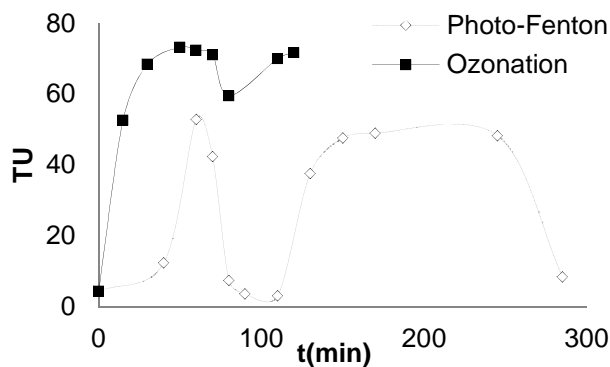


Figure 1. Toxicity evolution for the compared technologies.

Although ozonation was able to remove all the pesticide content, its mineralization was low and toxicity results were disappointed. Due to this and the advantages of photo-Fenton reaction regarding to its practical implementation -mainly abundance of iron species dissolved in agricultural effluents and the possibility of using solar light as a source of radiation- this preliminary survey lead to choose photo-Fenton reaction as the process to study, focusing the next step to its optimization and improvement of its efficiency.

EXPERIMENTAL DESIGN APPLIED TO PHOTO-FENTON TREATMENT OF HIGHLY METHOMYL-CONCENTRATED WATER

Appendix II, (Micó et al. 2010a), proposed the use of experimental design techniques to improve the efficiency of photo-Fenton for the depollution of methomyl containing effluents. The main objective of this work was to use the statistical information derived from the analysis of the experimental design to determine the most influential parameters of the process both evaluated responses, degradation of the pesticide load of the influent and increase intermediates biocompatibility. Biocompatibility starts in this point to be a crucial factor to be taken into account for the design of the integrated system.

In this phase of the process, high concentrations of the pesticide were still used. The experiments were performed according to a central composite distribution consisting on

a factorial design and 6 star points. Methomyl, hydrogen peroxide and ferric ion initial concentration were taken into account as main variables, being aware that there are many other factors that can interfere in photo-Fenton reaction, such as pH or temperature. Nevertheless these factors were fixed around the values expected in the field.

Extreme values for the involved parameters were the following [50, 200] mg·L⁻¹ of methomyl, [50, 100] mg·L⁻¹ of ferric ion and [100, 300] mg·L⁻¹ of hydrogen peroxide. Previous experiments revealed that peroxide concentration higher than 300 mg·L⁻¹ (close to the stoichiometric concentration needed to complete oxidation of 200 mg·L⁻¹ of methomyl as a pure substance) showed worse reaction yields, probably caused by a radical scavenging effect of the peroxide itself (Evgenidou et al. 2007). Interferences of the commercial excipients were discarded given that most of the total formulation was ethanol, which is resistant to react with hydroxyl radical regarding previous results not shown here. On the other hand catalytic inactivity of Fe²⁺ at lower concentrations than 50 mg·L⁻¹ was observed (in the presence of such high pesticide concentration); most likely due to the formation of complexes with any excipient of the commercial product, or pesticide metabolites as it happens with different organic compounds and dissolved iron species (Perdue et al. 1976). A mathematical model could be determined, based on table 1 from Appendix II:

$$Y(\%) = 45.2 - 0.6[Met.]_0 + 0.24[H_2O_2]_0 + 1.42[Fe^{2+}]_0 + 0.0009[Met.]_0[H_2O_2]_0 - 0.001[H_2O_2]_0[Fe^{2+}]_0 + 9.1 \cdot 10^{-4}[Met.]_0^2 - 4.1 \cdot 10^{-4}[H_2O_2]_0^2 - 0.001[Fe^{2+}]_0^2$$

r. 1

Applying ANOVA test to the results, initial methomyl concentration was shown as the first most influential parameter that determines maximum pesticide depletion. Apart from the target specie content by itself, the inert ingredients also contained the commercial formulation also interfere in the reaction due to the fact that they can be a source of radical consumption, in detriment of the pesticide degradation. The initial concentration of hydrogen peroxide was the second more important parameter while iron initial concentration is not mathematical significant. However this factor cannot be taken out from the model due to its cross effects and its quadratic value are indeed significant.

Regarding to the curvature of the response surfaces shown in fig. 1 of Appendix II for highest values of initial concentration of methomyl highest depletion percentages was achieved for highest concentration of reagents. Nevertheless, for the lowest concentration of pesticide, an optimum ratio for maximum pesticide depletion was calculated around intermediate values [Met]₀ = 50 mg·L⁻¹, [H₂O₂]₀ = 245mg·L⁻¹, [Fe²⁺]₀ = 77 mg·L⁻¹. The fact that the optimum is found in the intermediate region suggests that the existence of a scavenging effect for higher hydrogen peroxide concentration. As the optimum H₂O₂ concentration is much higher than the stoichiometric need of 50 mg·L⁻¹ of the pesticide itself, stating the influence of the inert ingredients related to the

optimum reagents value. This encourages the use of commercial formulation to subsequent studies regarding the fact that the contribution of inert ingredients must to be taken into account.

ANOVA results over biodegradability values showed that again the most influential parameter was the content of the pesticide, as was suggested in the first consideration. The interaction between the pesticide and hydrogen peroxide was the next more significant term, followed by the quadratic effects of hydrogen peroxide, ferrous ion and the direct effect of hydrogen peroxide. According to this, the equation that defines BOD₅/COD is presented as equation 37.

$$BOD_5/COD = -0.14 - 0.0018[Met.]_0 + 0.005[H_2O_2]_0 + 0.006[Fe^{2+}]_0 + 5.73 \cdot 10^{-6}[Met.]_0^2 - 5 \cdot 10^{-6}[Met.]_0[H_2O_2]_0 - 6[H_2O_2]_0^2 \quad r. 2$$

The influence of pesticide initial concentration and its quadratic term evident just with a sight to the whole group of biodegradability results performed in the study. It could be observed that biodegradability values for the highest concentrations of pesticide experiments are very low. As can be seen in table 29, on one hand there is the obvious high COD value inherent to a higher initial presence of pesticide, inert ingredients that photo-Fenton reaction is not able to totally mineralize. On the other hand and inhibitory effect to biodegradation can take place by methomyl itself, the inert ingredients or their metabolites. This effect seems to diminish in the cases with lower initial concentration of the pesticide, in which BOD₅ results are much higher but photo-Fenton process is also able to almost eliminate the whole methomyl content. In some of these cases, biodegradability values are close to 0.4, which characterizes easily biodegradable effluents (Sarria et al. 2002).

Table 1. Central composite design of photo-Fenton oxidation of methomyl commercial formula and corresponding results obtained for biodegradability parameters not shown in the paper.

#	([Met] ₀ , [H ₂ O ₂] ₀ , [Fe ²⁺] ₀) (mg·L ⁻¹)	BOD ₅ (mg O ₂ ·L ⁻¹)	COD (mg O ₂ ·L ⁻¹)	BOD ₅ /COD
1	50,100, 50	49.7	329.5	0.151
2	200, 100, 50	4.6	500.8	0.010
3	50, 300, 50	43.6	133.3	0.327
4	200, 300, 50	3.5	517.1	0.007
5	50, 100, 100	47.5	133.6	0.110
6	200, 100, 100	2.5	489.7	0.005
7	50, 300, 100	44.2	182.2	0.242
8	200, 300, 100	3.5	267.5	0.013
9	125, 26.79, 75	2.5	642.8	0.003
10	125, 373.71, 75	5.0	520.5	0.010
11	125, 200, 31.7	3.5	594.1	0.006
12	125, 200, 118.5	3.5	620.2	0.006
13	50, 200, 75	39.5	192.5	0.205
14	254.9, 200, 75	1.5	1321.2	0.001
15	125, 200, 75	42.5	298.8	0.140
16	125, 200, 75	45.0	386.5	0.120
17	125, 200, 75	29.5	270.4	0.110

Optimizing the mathematical expression, a trio of best initial conditions could be found, corresponding to a maximum biocompatibility of the final effluent; $[\text{Met.}]_0=50 \text{ mg}\cdot\text{L}^{-1}$, $[\text{H}_2\text{O}_2]_0=309.1 \text{ mg}\cdot\text{L}^{-1}$ and $[\text{Fe}^{2+}]_0=71 \text{ mg}\cdot\text{L}^{-1}$. This optimum was quite close to the optimum point regarding pesticide depletion, (50, 254, 77) $\text{mg}\cdot\text{L}^{-1}$. This coincidence establishes a relationship between the level of methomyl degradation achieved and the biocompatibility of the treatment final effluent, and states the importance of limiting the concentration of pesticide treated. This fact should be taken into account in the design of the separation stage. Its performance should provide the system with an enriched effluent, although its concentration should not exceed a certain value.

Regarding to the possibility of implementing a subsequent biological reactor to oxidize the organic matter non degraded by the process, the set of conditions for the maximal degradation showed a mathematically calculated biodegradability of 0.45, more than acceptable for considering the effluent as biodegradable (Sarria et al. 2002).

PHOTO-FENTON REACTION APPLIED TO IMIDACLOPRID HIGHLY POLLUTED WATER REMOVAL: STUDY OF PHOTO-FENTON PERFORMANCE

Appendix III, (Micó et al. 2009), covers works from the three stages described in the presentation of this chapter. It starts with the study of photo-Fenton performance over commercial imidacloprid polluted waters depending on the quantity of reagents added to the reaction. It is followed by the essays of the biocompatibility of the resultant effluents by the behavior of sequencing batch reactors fed with those wastes. Finally, the study is concluded with the use of molecular biology tools to determine the population distribution in some of those bioreactors, although this part was not included in the referred paper though will be explained in the corresponding section of this chapter.

For this section the main results regarding to photo-Fenton performance will be referred, including further work not included in the annexed paper.

The effluent to treat in this case was simulated by means of $20 \text{ mg}\cdot\text{L}^{-1}$ solution of imidacloprid, but in order to work in a more real scenario the pesticide was not used as pure specie (Segura et al. 2008), but as a commercial formula, as in the rest of the thesis work. Its composition contained $200 \text{ g}\cdot\text{L}^{-1}$ of imidacloprid as active ingredient. The so-called *non-active* or *inert* ingredients of the commercial formulation, dimethyl sulfoxide and propylene carbonate, are presupposed to cause interferences along the process, which could not be observed nor taken into account while working with the pure substance.

All the photo-Fenton reactions were carried out with $20 \text{ mg}\cdot\text{L}^{-1}$ imidacloprid as initial pesticide concentration and $15 \text{ mg}\cdot\text{L}^{-1}$ of Fe^{2+} . It was detected that although the expected TOC for those solutions was $8.45 \text{ mgC}\cdot\text{L}^{-1}$, the experimental value obtained was $47 \text{ mgC}\cdot\text{L}^{-1}$, implying a high contribution on carbonic matter by the inert ingredients, which could interfere with the reaction consuming free radicals themselves.

As can be observed in fig. 2 from Appendix III the degradation of the pesticide improved from 25 to 75 mg·L⁻¹ of hydrogen peroxide. While in the first case the final elimination reaches less than 70% of the total concentration, the depletion is total for 75 mg·L⁻¹. However, from that point, increasing the initial concentration of the reagent does not lead to faster pesticide degradation. In fact, highest peroxide concentration generates a longer degradation profile. This could indicate the existence of a scavenging effect by hydrogen peroxide, which is favored with higher [Fe²⁺]₀ / [H₂O₂]₀ ratio, as is the case. Hydrogen peroxide consumes radicals in detriment of imidacloprid degradation producing the formation of hydroperoxyl radical (·O₂H), much less reactive (Legrini et al. 1993). Quite drastic depletion of the pesticides on the first minutes can be seen. After those first minutes, generated by-products compete with the pesticide for the radicals and slow down its degradation rate.

Biodegradability measurements (BOD₅/COD) followed a similar behaviour as pesticide depletion, as can be seen in fig. 42. Biodegradability increases even with the softer treatment, showing how photo-Fenton reaction increases biocompatibility of the raw effluent. Nevertheless, the value obtained for the experiment with 75 mg·L⁻¹ is not improved with the increase of the reagent. The hypothetical scavenging effect of hydrogen peroxide could prevent the degradation of certain substances towards more biodegradable species.

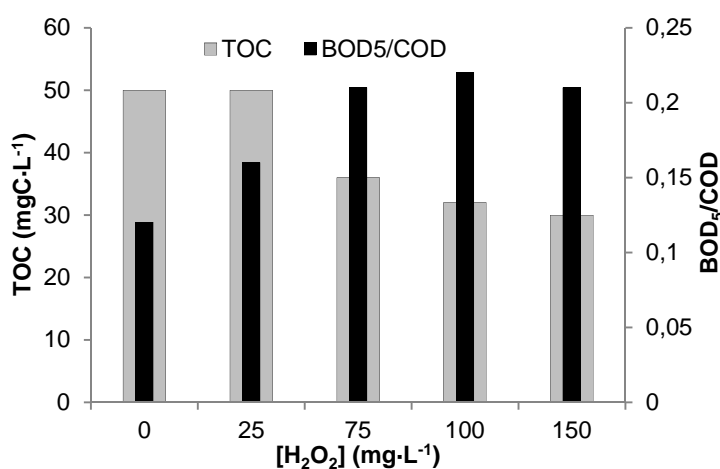


Figure 2. BOD₅/COD and final TOC results for different photo-Fenton treatments and an effluent just spiked with imidacloprid. [Imid.]₀=20 mg·L⁻¹, [Fe²⁺]=15 mg·L⁻¹.

In opposition to all this, better TOC depletion results were obtained for higher reagent concentrations. The best elimination share is reached by the processes with peroxide concentrations of 100 and 150 mg·L⁻¹, with nearly a 40% of TOC diminishment. Despite the total depletion of imidacloprid is achieved for those high peroxide doses, complete mineralization is not obtained in any case. One of the reasons could be the consumption of hydroxyl radicals by H₂O₂, which prevents them from contributing to the mineralization. The other reason could be the formation of recalcitrant by-products, not susceptible of being oxidized in the conditions in which the reaction was carried out.

It is also noticeable how TOC depletion is higher for higher peroxide doses, in opposition to what is expected if scavenging effect is indeed taking place. A plausible explanation could be that the scavenging effect is compensated regarding to organic matter depletion by a certain higher affinity for hydroxyl radicals of the inert ingredients or generated by-products. Those species compete with H_2O_2 for the scavenging of the radicals setting back the degradation of imidacloprid, but not enough for promoting the mineralization of the load.

FOSETYL-AL PHOTO-FENTON DEGRADATION AND ITS ENDOGENOUS CATALYST INHIBITION

Appendices IV and **V**, (Micó et al. 2013b) and (Micó et al. 2013a), are focused on the interferences and inhibitory effects that can affect photo-Fenton reaction by the presence and activity of different species in the reaction media.

In the case of **Appendix IV**, the studied interferences are those generated during the oxidation of organophosphorous fungicide fosetyl-Al. Due to its structure, the oxidation of this pesticide releases to the reaction media phosphate salts that scavenge iron and hinder Fe (II) availability by precipitating extremely insoluble $FePO_4$.

According to this, the main aim of this study was to evaluate the effect of this catalyst inhibition affecting fosetyl own degradation and the oxidation of other pesticides coexisting in a mixture. For this purpose experimental design in an artificially enlightened reactor was used, followed with biodegradability tests. Also solar photo-Fenton experiments were carried out in relation to the results obtained from the experimental design in order to complete the picture. The low organic content of fosetyl-Al commercial formulation justifies the low doses of hydrogen peroxide and iron, compared to previously commented works.

Regarding to the structure of the studied fungicide, shown at the Introduction, the main specie to blame for any photo-Fenton inhibitory effect is phosphate. This anion, which is released to the media as fosetyl is oxidized, is supposed to precipitate Fe^{3+} as $FePO_4$. This fact knocks out ferric ion which is no longer available for the photo-reduction that would send it back to the photo-Fenton cycle. An indirect proof of the existence of this inhibition process and its importance was given by the analysis of the experimental design results. Mathematical models obtained for two crucial variables as the pesticide half-life and biodegradability showed how iron concentration was among their most significant parameters. Therefore, any scavenging effect exerted to that specie would jeopardize both answer, and the precipitation of phosphate salts will do.

Nevertheless, the monitoring of different experiments whose how phosphate concentration profile during reaction was not as easy to understand as expected. On one hand, despite fosetyl seems to be quickly degraded, corresponding phosphates (3 times initial molarity of the fungicide) were not released to the media the same rate, but gradually, during the first minutes of the reaction. Furthermore, the small fraction of

total iron concentration reduced during those first minutes cannot be blamed for the precipitation of all the missing phosphates. On the other hand, despite it was seen how Fe(II) is rapidly converted into Fe(III) also on the first minutes of the reaction, what released to the media plenty of ferric ion, it did not seem to rapidly precipitate with available phosphate.

Both factors made the authors think that there was a relative complex chemistry regarding to phosphate and iron species in the reaction media. Fig. 43, also seen in Appendix IV pretends to simplify the main roles of every part related to that chemistry.

Fosetyl saturated carbon bonds suggest that the main reaction mechanism with hydroxyl radicals will run through hydrogen abstraction followed by a subsequent possible formation of phosphate containing polymeric by-products, $(\text{PO}_4^{3-})_n\text{-R}_m$ (Samuni and Neta 1973). Only through the advance on the oxidation these species end up decomposing and releasing PO_4^{3-} to the media. This will explain the delay in the release of phosphates at the beginning of the reaction.

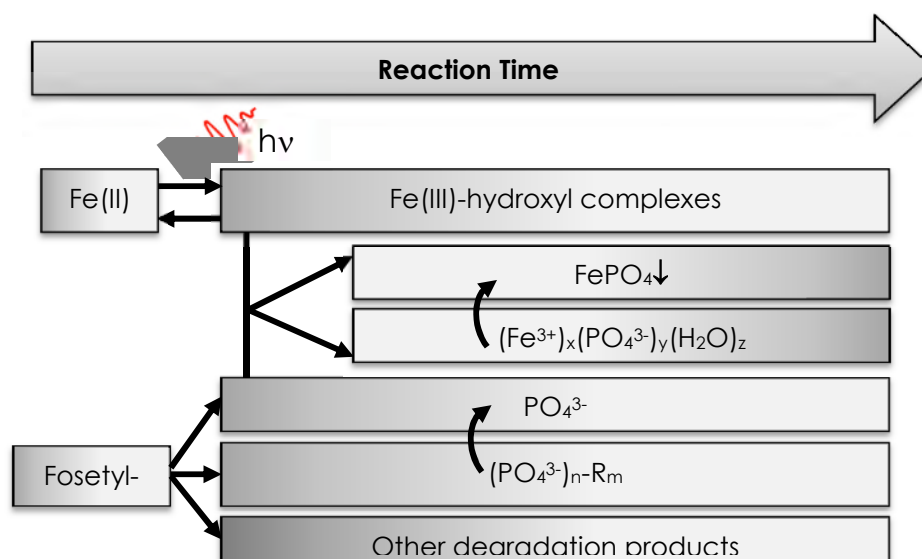


Figure 3. Schematic figure of the chemical evolution of iron and phosphate species during photo-Fenton reaction. $(\text{Fe}^{3+})_x(\text{PO}_4^{3-})_y(\text{H}_2\text{O})_z$ refers to complexes proposed, while $(\text{PO}_4^{3-})_n\text{-R}_m$ stands degradation phosphate containing degradation by-products.

According to Pignatello (Pignatello et al. 2006), in the conditions of the reaction, Fe (III) is not usually free in the solution, but tends to form hydroxyl complexes, soluble and photoactive. Although it was expected that the presence of phosphate ions would decompose these complexes for the iron precipitate, what could be happen is that the formation of another kind of complexes are taking place, precisely involving (PO_4^{3-}) . They are formed by the interaction between Fe(III), water and phosphates (Lente et al. 2000), $(\text{Fe}^{3+})_x(\text{PO}_4^{3-})_y(\text{H}_2\text{O})_z$, and impede phosphate salt precipitation.

The applicability of solar light to enhance the decontamination of fosetyl-Al was also essayed. And it was evident how the fastest experiments were those made under solar radiation, encouraging the use of this source of light to empower photo-Fenton reaction in real applications. The higher light incidence intensity over the solar device (between

17 to 25 $\text{W}\cdot\text{m}^{-2}$, in front of around 7 in $\text{W}\cdot\text{m}^{-2}$ for the UV lamps device), together with possible photo-chemical reactions that would undergo beneath the visible range of solar light spectrum, could justify the increase in fosetyl-Al degradation velocities in the case of sun powered photo-Fenton, in opposition to UV lamp process.

A mixture of three studied pesticides was also submitted to solar photo-Fenton. The differentiation on the elimination rate of each compound highlighted that, even though hydroxyl radical, in which is based this technology, does not react selectively with organic matter, it does it indeed with different initial degradation rate, depending on the structure of the oxidized molecule (Walling 1975). Nevertheless the most interesting results obtained in this essay were the uncompleted elimination of every species, and the shape of the degradation profiles. In previous works with methomyl and imidacloprid treated separately (**Appendix II** and **III**), and combined (**Appendix V**), their profiles always presented a gradual concentration decrease from the very beginning of the process. This revealed the existence of a competition for the radicals between pesticide species (and/or their inert ingredients and by-products).

The main conclusions of this work could be that photo-Fenton seems to be an effective way of treating pesticides solutions containing fosetyl-Al. Its solar version is even more effective than UV light powered process, which is an advantage due to the use of an inexpensive source of radiation. It has been stated that fosetyl containing effluents compose cases in which endogenous inhibition should be taken into account, and the optimization of the working conditions is extremely troubled by it. In this case, regarding to multivariate analysis results and in opposition to what was expected, the concentration of the catalyzer (affected by fosetyl degradation) seemed to be more influential than the oxidant agent itself.

ENHANCEMENT OF PESTICIDE PHOTO-FENTON OXIDATION AT HIGH SALINITIES.- STUDY OF COMPLEX MATRIX EFFECT ON REACTION

Appendix V, (Micó et al. 2013a), presents the work related to the interferences caused by the matrix of salts that composes the effluent to treat. It tries to resemble as much as possible to the real streams from the hydroponics greenhouse after its maximum recycling and after its pass through the membrane separation system, which brine is sent to be treated by photo-Fenton reaction.

Salinity effect over pesticide depletion

Inorganic ions, such as NO_3^- , SO_4^{2-} and Cl^- , are known to cause interferences in the photo-Fenton reaction (Bacardit et al. 2007; Bourgin et al. 2011; Kitsiou et al. 2009; Maciel et al. 2004; Siedlecka and Stepnowski 2006), what usually hinder oxidation results. These anions could be blamed for a scavenging of hydroxyl radicals (Bacardit et al. 2007; Lipczynska-Kochany et al. 1995; Pignatello et al. 2006); and for complexation with dissolved Fe(III), forming less photoactive species (Pignatello et al. 2006). In order

to monitor both effect, several photo-Fenton reaction were carried out at different salinity conditions, from the absence of added salts to concentration of $42.13 \text{ g}\cdot\text{L}^{-1}$ ($50 \text{ mS}\cdot\text{cm}^{-1}$, simulates reverse osmosis concentrate).

In opposition to what was expected, results shown how salinity, mainly represented by Cl^- , has a positive effect over pesticide depletion, or at least does not jeopardize its oxidation. Even for the highest conductivities.

Under certain conditions, halogen reactive species may participate in contaminant destruction by the formation of monoatomic halogen atoms $\text{X}\cdot$, which rate constants with organic compounds are comparable to those for $\text{OH}\cdot$ (Grebel et al. 2010). The participation of this type of radicals could justify the improvement of methomyl and imidacloprid depletion and even the changes in their profiles. Furthermore, due to the molecular formula of methomyl, chloride radicals could promote the formation of extremely nucleophilic compounds that could even collaborate in the oxidative process, as outlined in fig. 44.

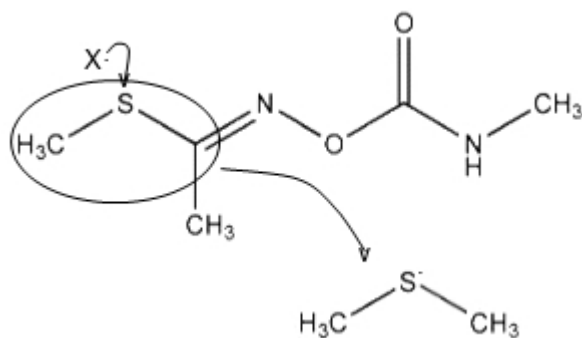


Figure 4. Simplified generation of the possible nucleophile degradation product.

In the case of imidacloprid, the improvement is more subtle or even negligible, due to its molecular structure, mainly its pyridine ring, fig. 45, which tends to stabilize any type of radical instead of promoting the expected chain reactions.

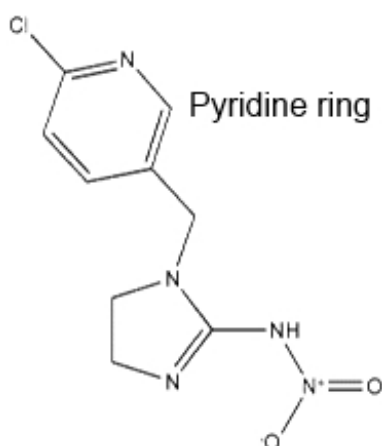


Figure 5. Identification of the pyridine ring.

Interferences over iron availability

A general behavior can be distinguished among iron species for the different experiments. Ferrous ion suffers an extreme decrease when the hydrogen peroxide is added to the media, no matter the conductivity of the effluent, and its concentration is kept low during the process until 70-80% of the peroxide is consumed, coinciding with the lowest remaining concentrations of the pesticides. A recovery on Fe (II) could be observed at the end of the reactions.

These experiments results enable the creation of a scheme summarized in fig. 46, also seen in **Appendix V**. At the beginning a quick reaction between hydrogen peroxide and ferrous iron takes place, causing the oxidation of the last one and the generation of radicals, it corresponds to dark Fenton reaction. From that point, all depicted reactions are expected to happen constantly throughout the photo-Fenton process; however, there may be, as in this case, other complexing reactions that disable Fe^{3+} from participating in this cycle as efficiently as expected.

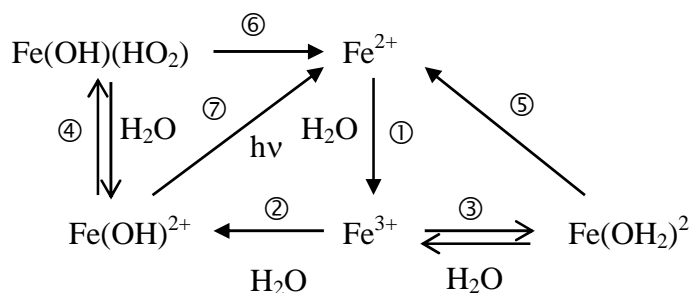


Figure 6: Simplified diagram of iron cations chemistry. Reactions are not balanced. Reaction 2 is representative of the several complexing reactions that take place between Fe(III) and water.

As it was already mentioned, inorganic ions are known to exert some coordinating effect over ferric ions (Pignatello et al. 2006), with the formation of thermodynamically favored complexes such as FeCl_2^+ , FeCl_2^+ and $\text{Fe(SO}_4)_2^-$, reducing the capability of the photo-Fenton reaction to recycle ferrous iron (Millero et al. 1995). However, it is also known that Fe(III) may also complex with certain organic compounds (Nichela et al. 2010), especially those acting as polydentate ligands, which would explain the low levels of dissolved Fe(II) until nearly the end of the trials. Performed experiments stated how methomyl or its inert ingredients can complex ferric iron to a certain grade. On the other hand, even in the case of salts' absence, it was also seen how imidacloprid commercial formulation prevents Fe(III) photo-reduction. No complexing effect can be attributed to the organic solvents that the commercial formulation contains. Instead, is again the pyridine ring that could provoke the chelating effect over ferric ions (Constable 1990). This ring is unharmed during the first stages of the degradation of the compound (Kitsiou et al. 2009). However, with the evolution of the reaction, this cycle is also decarboxyted and decomposed by the produced radicals, promoting the regeneration of a slightly higher concentration of Fe(II) that could be seen at the end of every reaction.

Appendix V main conclusions could be summarized stating that salinity content does not hinder pesticide depletion by photo-Fenton reaction, but can enhance it in certain cases. Despite that, a certain inhibition of iron catalytic activity is taking part at the

same time, thanks to the salts content but also to the organic matrix of the effluent to treat.

4.2. BIOREACTORS

PHOTO-FENTON REACTION APPLIED TO IMIDACLOPRID HIGHLY POLLUTED WATER REMOVAL: STUDY OF EFFLUENTS BIOCOMPATIBILITY

Appendix III, (Micó et al. 2009), showed BOD₅/COD ratios achieved in photo-Fenton experiments quite lower from what is considered readily biodegradable, according to (Sarria et al. 2002). However, previous experiences, not described here, stated that those values were enough to try the integration of a subsequent bioreactor.

To prove that, a set of four 1 L sequencing batch reactors were displayed under O₂ saturation and continuous stirring conditions by means of an air bubbling system and several magnetic stirrers. Three of the samples to assess were each final effluent of photo-Fenton reactions, performed as described before, with the photo-Fenton resultant remaining content on imidacloprid, by-products and inert ingredients. The fourth one was a non-treated dilution of imidacloprid, essayed to evaluate the biodegradability of the commercial formula itself. Table 30 gathers the initial properties of four reaction mixtures, for the adaptation and the second cycles.

Table 2. With subindex 0, initial conditions of photo-Fenton, pH=2.7. With subindex R, second cycle initial conditions inside the reactors, in terms of pesticide concentration, TOC and suspended volatile solids, once the load was carried out.

Sample	[Imid.] ₀ (mg·L ⁻¹)	[Fe ²⁺] ₀ (mg·L ⁻¹)	[H ₂ O ₂] ₀ (mg·L ⁻¹)	[Imid.] _R (mg·L ⁻¹)	TOC _R (mgC·L ⁻¹)	TVSS _R (mg·L ⁻¹)
A	20	-	-	22.1	51.4	360
B	20	15	25	14.8	51.8	240
C	20	15	50	5.0	42.1	240
D	20	15	100	0.1	33.9	210

After a period of biomass adaptation (first cycle), while TOC experimented an irregular behaviour with increases and decreases and later reaching a stable value for all four reactors (results not shown here), a second cycle was set recovering by sedimentation the remaining biomass from every reactor and loading the same mixture as in the previous round. This indicated that biocompatibility of the effluents were indeed enough to keep the activity of the biomass of a subsequent bioreactor.

Figs. 47a and 47b show the evolution of pesticide concentration and Total Organic Carbon content along the biological digestion during the second cycle.

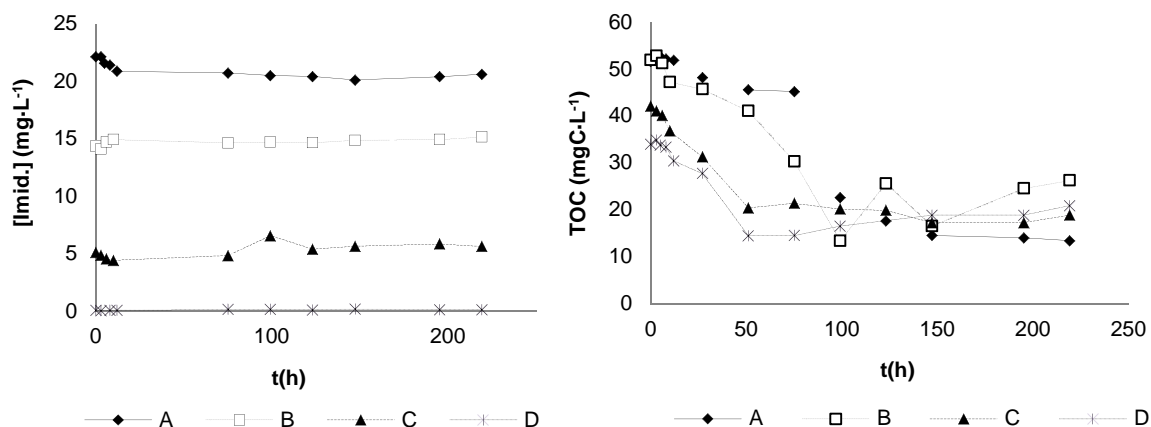


Figure 7. 47a. Profile of imidacloprid concentration in the biological reactors. 47b. TOC depletion curves for the different loads.

As can be seen, in fig. 47a, the biological degradation of imidacloprid is nearly negligible, not only for the highest concentrated non pre-treated load but also for the treated ones, this fact states the biological recalcitrance of this neonicotinoid. This implies that the real biodegradable content of the samples evaluated in both biological tests does not come from the pesticide itself, but the by-product and inert ingredients also contained in the effluents. Fig. 47b shows the progressive depletion of total organic carbon. TOC descends noticeably in two days for the loads C and D. For loads A and B, with higher initial concentrations, the decrease is delayed, suggesting an inhibitory effect due to the pesticide, but also came to a minimum that remains constant till the last days of the essay, representing a refractory organic fraction remaining after chemical-biological treatment, from 13.00 to 27.00 mgC·L⁻¹.

The resistance of imidacloprid to biological degradation, together with the evidence of the existence of an organic load not decayed by the chemical treatment but noticeably reduced by the biological one, would justify the need of a coupled chemical-biological treatment against this kind of pesticide on the initial concentration studied in this work. The AOP is able to diminish the quantity of pesticide in the effluent, but the pollutant load remains in the shape of metabolites and inert ingredients (probably unharmed after the photo-Fenton process), which is reflected on the low decrease of TOC after the chemical treatment. About biological treatment itself, though the bioassays were not able to cope with the neonicotinoid depletion, their capability to degrade the organic load becomes evident, at least till arriving to a residual TOC concentration that can be considered acceptable for this kind of process. The optimization of photo-Fenton reaction could reduce reagents if it is focused just in the depletion of the toxic load, while a subsequent well designed bioreactor could diminish the rest of the organic matter.

Apart from attesting the need of a coupled system, these results revealed how useful sequencing batch reactor tests could be for the characterization of the effluent biocompatibility. Although BOD₅/COD stated a certain grade of biodegradability, batch bioassays have shown that it was not due to imidacloprid itself (that has been proved as

biorecalcitrant) but to the accompanying non-active ingredients, indicating the partiality of the information derived just from BOD₅/COD assays.

SLOW SAND FILTRATION AS PART OF AN INTEGRATED SYSTEM FOR PESTICIDES REMOVAL IN HIGH SALINITY EFFLUENTS: BIOREACTORS PERFORMANCE

Appendix VI, (Micó et al. 2013a), pretends to study the suitability of the integration between photo-Fenton reaction and a slow sand filtration column to treat pesticide contaminated effluents, as proposed in this thesis, at different salinity conditions. These results will show if the proposed coupled system could be a treatment option for the strategies proposed at the CENIT-MEDIODIA Project of this thesis: if the system will be proficient to treat the discarded current from the recycling ($\sim 10 \text{ mS}\cdot\text{cm}^{-1}$), or even to process the concentrate of a reverse osmosis stage, which would reduce the volume of the discarded effluent ($< 50 \text{ mS}\cdot\text{cm}^{-1}$).

This study comprises a first step in which the biodegradability of the different effluents, based on results from (Micó et al. 2013c) are tested by means of monitoring the performance of sequencing batch reactors (SBR). On the second step, photo-Fenton final effluents are loaded to the slow sand filtration column. Its performance is monitored to verify that the integration between the chemical process and the bioreactor is robust enough to be efficient for different salinity values.

Bacterial 16S rRNA gene sequencing will be also applied to analyze microbial diversity of the biomass layer, schmutzdecke. However, those results will be explained in next subsection.

Sequencing batch reactors

Six 1L Erlenmeyer flasks were filled with 900mL of the effluent to process and 100 mL of secondary liquor from WWTP, in Gavá, Barcelona. Table 31 summarizes their most important parameters.

	BC	B0	B1	B2	B3	B4
Conductivity ($\text{mS}\cdot\text{cm}^{-1}$)	0.015	0.015	1.00	5.06	11.06	50.00
DOC₀ ($\text{mg}\cdot\text{L}^{-1}$)	45.19	35.76	39.57	41.15	42.24	43.51
[Imid.] ($\text{mg}\cdot\text{L}^{-1}$)	10	0.01	0.03	0.03	0.13	0.77
[Met.] ($\text{mg}\cdot\text{L}^{-1}$)	10	Not detectable	0.01	0.05	Not detectable	Not detectable
$\Delta\text{DOC}_{1\text{st cycle}}$ (%)	72.6	60.1	65.2	69.8	69.5	71.5
$\Delta\text{DOC}_{4\text{th cycle}}$ (%)	72.4	74.5	78.2	81.8	85.2	82.3

Table 3. Relevant values for the different SSBs.

Two main issues could jeopardize the performance of these biosystems: On one hand, given that the inoculum came from a regular treatment plant and the volumetric ratio is as high as 90%, in the cases of higher salinities, osmotic shock could collapse those bioreactors or hinder the metabolism and development of the biomass. The osmotic

stress takes place when a sudden change in salinity (and other solutes concentrations) happens around the cell, causing a rapid change on the flux of water through cell membrane (in order to equilibrate higher conductivity in the surroundings). This variation can obstruct or inhibit the proper transport of nutrients and cofactors into the cell, causing it to shrink and collapse (or to swell and burst, when the concentration outside the cell is too low) that may end up in cell death.

On the other hand, the toxicity of the pesticide content, its inert ingredients or the by-products generated during photo-oxidation process. Potential cytotoxicity of the effluents, specially expected in the case of the non-treated effluent (BC reactor), could cause different effects over the biomass, from cell necrosis, to cell lysis, to inhibition of its duplication.

However none of these phenomena jeopardized the performance of sequence batch reactors, given that they showed a good response regarding to DOC depletion from the very first cycle.

This first cycle performance could be considered an indication of the presence of a readily biodegradable fraction in every case. DOC depletion in this cycle, between 60 to 70% for every bioreactor, and the evolution of VSS highlighted the resistance to the osmotic pressure of the effluents and their potential toxic content.

For the rests of the cycles, noticeably high DOC depletion was also observed for every case, increasing with every cycle, especially for reactors from B0 to B4, indicated how the biological reactors overcome any probable salinity and toxicity problems and are able to mineralized an important amount of dissolved organic carbon. The elimination percentage is higher for those treated loaded bioreactors than for BC reactor, indicating the photo-Fenton reaction contributes to increase biodegradability of the loads.

Regarding to VSS, in the first cycle, their values slightly decrease after a short adaptation lapse but gave no hints of the collapse of the system, but of the evolution and acclimation of the microbial population of inoculated biomass. However in almost every reactor it could be seen how after that initial descent, a slow augmentation takes place with the advance of the second cycle, indicating again the effective acclimation of the biomass. This adaptation justifies the improvement of DOC depletion, even in the circumstances of extreme salinity of B4. However, in every case, there is a remaining fraction of DOC non-biodegradable, but in the last cycle, this is lower for the pretreated loads.

Another negative issue was also observed. In reactors were the presence of pesticide could still be detected (due to the performance of photo-Fenton or to the lack of pretreatment), no depletion of these xenobiotics took place. On one hand this reflects biorecalcitrance of methomyl and imidacloprid. On the other, it states the lack of evidence of an inhibitory effect by these substances, as said, given the performance of the biomass according to the good metabolizing results. According to this, it would be important to keep in mind that although bioreactors can considerably diminish organic content, the pesticide load can pass through them unharmed, with the environmental risk

it entails. This is why the application of an optimized chemical pretreatment cannot be avoided.

To summarize, it could be concluded that photo-Fenton and a subsequent biotreatment is a promising way of eliminate the pollutant load of high salinity greenhouse leachates containing pesticides. While photo-Fenton reaction could be optimized for the total removal of the pesticides, bioreactors are able to cope with the remaining organic load with effluents with high conductivity. All this suggest that also good results could be expected for slow sand filtration column.

Slow Sand filtration column

To begin with the operation of the slow sand filtration column, 2 L of chemically pre-treated effluents from type 1, neutralized with KOH, was mixed with 1L of sewage from secondary treatment. This mixture was oxygenated to a DO concentration of $8.5 \text{ mgO}_2 \cdot \text{L}^{-1}$, then it was continuously recirculated, supplying oxygen when needed, during 48 h.

After that period, the recycling system was open and the feed was renewed with 2 L of fresh KOH neutralized chemically pre-treated effluents load from type B1 (table 6), that were then persistently feed to the surface of the supernatant layer of the column by a peristaltic pump that dosed it by constant dripping. Samples were taken from the lowest outlet in order to monitor dissolve oxygen and measure DOC, pesticide content and concentrations of ammonia, nitrates and total nitrogen. The change between one load type to another was drastic in every case. The new effluent just substituted the old one once its last recharge was about to finish. For more details about the methods, see **Appendix VI**.

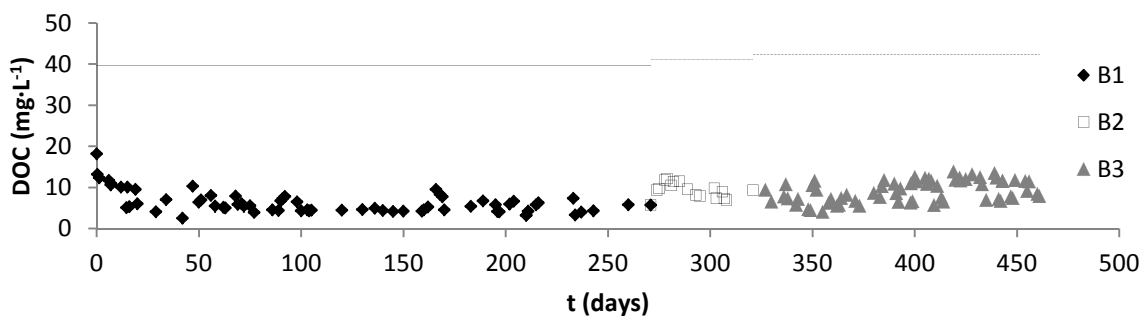


Figure 8. DOC evolution along slow sand filtration column performance. On the legend, B1, B2, B3 correspond to the type of effluent loaded in each different stage, see table 1. Upper lines indicate inlet DOC value.

Fig. 48 represents DOC measures for the different load stages of the column. It can be seen that from the very first moment, just a few hours of start of the process, DOC reduction is noticeable and it keeps diminishing till achieves values between 4 and 5 $\text{mgC} \cdot \text{L}^{-1}$. According to the assumption of no significant adsorption process is taking place, the existence of an established biomass could be assumed. This is confirmed by the fact that DO values at the column outlet for those first hours were around 2.3 and

1.2 mgO₂·L⁻¹, what points out the aerobic biodegradation of this organic matter, and the fact that this depletion does not take place just to a physical phenomenon of filtration.

Decreasing tendency is followed by the other two higher conductivities loads. Although DOC values are slightly higher than in the first period, achieved DOC depletion is around 75%, what indicates the capability of the schmutzdecke to metabolize the organic matter that remains after oxidation, even for the highest salinity condition tested. All this shows that the activity and development of microorganism population is able to metabolize a noticeable amount of organic matter present in Photo-Fenton effluents, an average of 30 mg·L⁻¹ related to every load DOC content, consuming 6.5 mg·L⁻¹ O₂ in the process. No osmotic shock was observed either, given that there were no stiff changes in the measured parameters for increased salinity. This quick adaptation and the resistance to relatively harsh conditions could be related to the fact that supported biomass is more resistant to adverse media conditions compared to suspended biomass reactors (Bishop, 1997; Shieh and Keenan, 1986), and confirms the performance response previously observed in the SBR's.

Although the nutrients were added fulfilling stoichiometric needs, in relation to the chemical oxygen demand (COD) income, no nitrification or denitrification seemed to take place significantly (TN, [NH₄⁺], [NO₃⁻] differences between inlet and outlet were negligible). That fact could be explained by the low levels of DO caused by organic matter biodegradation, together with the continuous low values of DOC disposal, precisely due to an intense biological oxidation. Furthermore in literature it is already stated that under normal design and operation, SSF are generally not capable of removing nitrogen (Amy, et al., 2006).

Pesticide degradation was not noticed either for the loading effluents B1 and B2 (in type B3 degradation of pesticide by photo-Fenton reaction was complete previous to the biological reactor). This indicates that if their concentration after photo-Fenton is not low enough for the public standards, it should be optimized for achieving higher depletions. However, the active presence of biomass indicates that remaining pesticides and metabolites do not inhibit its growing and the second can be mostly depleted.

Results just discussed were obtained analyzing samples acquired from the final sampling point of the column. In order to check the distribution of this biological activity along the column, samples from every outlet were also drawn and DOC and DO were measured. Results showed that most part of DOC consumption and DO decay takes place just before the first sampling point -only 15 cm under the surface of the solid- as can be seen in fig. 49. DO measurements also shown a noticeably drop from 7.5-8 mgO₂·L⁻¹ in the feeding tank to 2.5-1.8 mgO₂·L⁻¹ just in the first outlet, keeping similar values for the rest of them. All this makes evident that the biomass layer activity is mostly located on the first centimeters of the column, a fact that previous researchers have already stated (Campos, et al., 2002). This fact could suggest the need of the optimization of the filtering media depending on the characteristics of the load. High solid content in real effluents will require higher (or deeper) columns, while in the cases

where the requirements are more related to biomass activity, the column could be reduced.

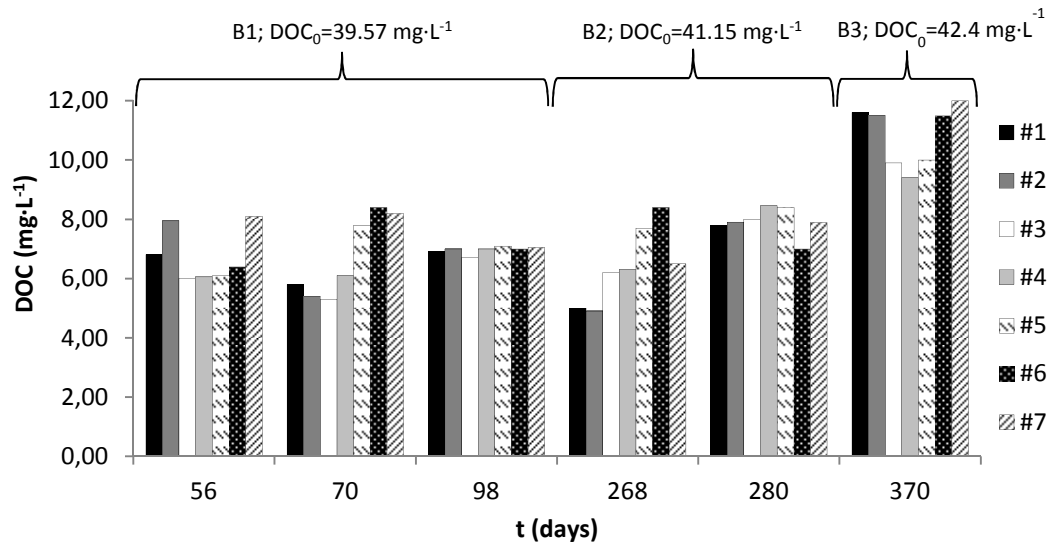


Figure 9. Representative DOC measures for samples taken from every outlet in a row. The first three correspond to the first period with $1.6 \text{ mS}\cdot\text{cm}^{-1}$ effluent, next two were taken during the period of $5.6 \text{ mS}\cdot\text{cm}^{-1}$ loading, and the last one belongs to the highest salinity concentration charge. Listed on the left, the number of the outlets, being #1 the closest to the surface and #7 the last one, from where samples were taken regularly.

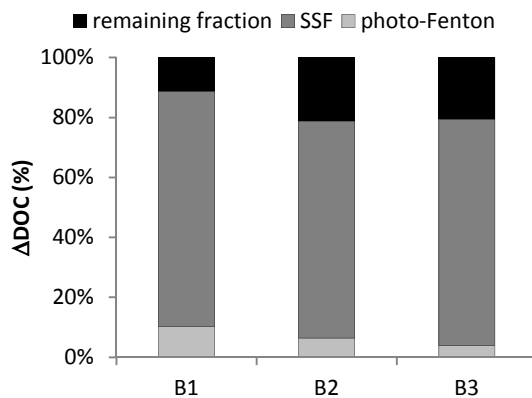


Figure 10. DOC depletion percentages for photo-Fenton and biological processes

Fig. 50 shows the contribution of each process to final DOC elimination. Mineralization achieved by the biological reactor is between a 72% and a 78%. B3 case is especially interesting given that although the mineralization grade by photo-Fenton reaction is very low, biomass was able to cope with 75% of the total organic content. In the case of SSF, the biorecalcitrant remaining fraction is lower for higher salinity values, which is also a very positive result towards the coupling.

4.3. MOLECULAR BIOLOGY TOOLS

PHOTO-FENTON REACTION APPLIED TO IMIDACLOPRID HIGHLY POLLUTED WATER REMOVAL: MOLECULAR BIOLOGY TOOLS

Appendix III, (Micó et al. 2009), results regarding to the characterization of the biomass from the sequencing batch reactors from are commented hereby. As was previously mentioned, these results were not part of the abstract sent to the congress (Micó et al. 2009), but more complete studies performed afterward.

The characterization of the bioreactor started with a previous work in order to choose the appropriate primers to perform sequencing process. The main characteristics that should be accomplished by the primers are: they should be bacteria specific; they should be complementary to DNA regions included inside the sequence replicated in the first PCR step, performed with the primers 8F, 1492R (see Chapter 3); primers should determine a manageable size sequence, between 100 and 200 bp (University of Michigan. DNA Sequencing Core), with enough hypervariability for genotyping-fingerprinting.

After a bibliography search, V3F and V3R, which correspond to a region V3, present in all bacteria, were chosen as the primers to use. A sequence homology search through already known sequences retrieved in prior works with other bioreactors (Esplugas 2010) was performed. As no alternative priming sites were found, apart from the target sites from V3 region, these two primers were used for sequencing. The use of these oligonucleotides, instead of inner vector primers, used as default, allowed obtaining more significant sequences.

Sludge samples were extracted from batch reactor D, characteristics shown in table 32, once its performance was stable. Molecular biology tools were used to study the microbial diversity in the media by 16S rRNA sequencing. The resulting bacterial distribution is shown in fig. 51, where the percentages of the different classes and phylums are represented.

Table 4. Effluent characteristics previous to being fed to sequenced batch reactor.

Sample	[Imid.] ₀ (mg·L ⁻¹)	[Fe ²⁺] ₀ (mg·L ⁻¹)	[H ₂ O ₂] ₀ (mg·L ⁻¹)	[Imid.] _R (mg·L ⁻¹)	TOC _R (mgC·L ⁻¹)	TVSS _R (mg·L ⁻¹)
D	20	15	100	0.1	33.9	210

As expected according to literature (Deng et al. 2012) and (Wagner and Loy 2002), the aerobic conditions of the reactors are related to the abundance of *Proteobacteria* (~45%) and *Bacteroidetes*, followed by *Acidobacteria* group and *Gemmatimonadetes* phylum, and, in lower proportion, *Planctomycetes*, *Actinobacteria* phylums and *Verrucomicrobia* group.

Proteobacteria comprises individuals from a wide range of functional clusters; from organic matter degraders, to denitrifiers and polyphosphorous-accumulating bacteria. Among this phylum, the most predominant class is *β-proteobacteria*, being *Rhodocyclales* (13.8%) its main representative. The closest reported microorganism to

these sequences was determined to be, *Methyloversatilis sp.*, with similarities between 99 to 95%. These organisms have been already identified as able to grow on single-carbon compounds (Kalyuzhnaya et al. 2006), in this case probably, metabolizing the partially mineralized organic load by the previous chemical treatment. *Hydrogenophilaceae* family is the second cluster in order of abundance among the β class, known as involved in H₂ metabolism, followed by *Burkholderiales*, efficient in the mineralization of dissolved organic matter (Niemi et al. 2009).

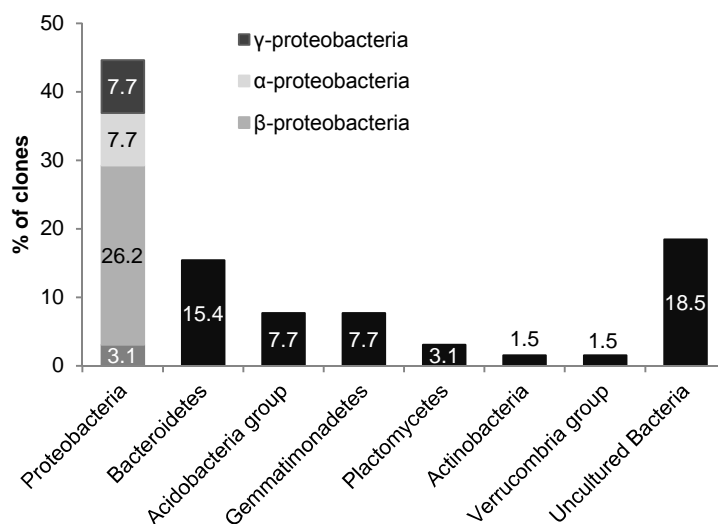


Figure 11. Percentage of the most abundant phylums and groups, with the breakdown of the phyla among the *Proteobacteria*.

α and γ -*proteobacteria* are less abundant, but each of them still represents around an 8% of the total population. Half of the retrieved sequences from α order were identified as *Sphingomonadales*, reported as main cause of biofouling in membrane-based processes (Calderón et al. 2011), being specially active in the segregation of exopolymer. One of the other clones affiliated to α order matched an organism from *Sinorhizobium* genus (Similarity 99%, GenBank: JN867346.1), reported as taking part in the degradation of neonicotinoid pesticide as our target compound is. Among γ -*proteobacteria*, *Pseudomonadales* are slightly more abundant than *Xanthomonadales* order. First has been detected inside a nicotine degrading consortium (Wang et al. 2009a), molecule with essential structural similarities with the target compound of this work. For its part, *Xanthomonadales* order is characterized by its *nirS* gene, typical of denitrifying bacteria. However no chemical testimony of related process could be found.

The second more important phylum is *Bacteroidetes*, which has been reported as able to degrade a variety of pollutants, playing important roles in wastewater treatment, (Deng et al. 2012) and (Xia et al. 2010). Among them, *Sphingobacteriia* is the most numerous class (6.2%), followed by *Cytophagia*, and a clone of *Flavobacteriales*, a polyphosphorous-accumulating bacteria (Deng et al. 2012).

Acidobacteria group and *Gemmatimonadetes* phylum are the next more abundant clusters. Most of the *Acidobacteria* clones matched with a similarity of 99% the Uncultured *Acidobacteria* bacterium clone C6_3 (GenBank: EF562546.1), reported as part of a stable microbial consortia capable of degrading complex organic matter. *Gemmatimonadetes* phylum is generally associated to soil cultures; nevertheless it has also been reported in the context of biological reactors (Patil et al. 2009) and (Wang et al. 2009a), related to N₂ cycle.

A high percentage of the retrieved clones (20%) could not be identified without any known taxon, which underlines the need for a more extensive molecular biology approach to study this type of ecosystem. However almost half of the uncultured bacteria matched the clone named Pohang-WWTP_October.2006_6203 (similarity 99%; GenBank:HQ509685.1), identified inside the bacterial community structure of an activated sludge process.

SLOW SAND FILTRATION AS PART OF AN INTEGRATED SYSTEM FOR PESTICIDES REMOVAL IN HIGH SALINITY EFFLUENTS: BIOMOLECULAR ASSESSMENTS

In **Appendix VI**, (Micó et al. 2013a), regarding to the performance of the SSF, the quick depletion of the organic load and dissolved oxygen after the first centimeters of the column, it could be assumed biomass was mainly established between the surface of the column and its first inlet, expanded clay samples from the middle point of this region were withdrawn at the end of every cycle. Those solids were grinded and submitted to DNA extraction. After this process, followed by cloning and sequencing, **Appendix VI** shows the characterization of the biomass grown in the column after its acclimation to the different loads. The handled samples had a particularity that forced to adapt the protocols used until that moment. The salinity content of the samples, especially for stages 2 and 3, showed difficulties at the first PCR step, inhibiting the replication reaction. Even after using a DNA cleaning procedure, the inhibition was high enough completely hinder PCR. However, a simpler solution seemed to solve the problem. Instead of directly using extraction product as DNA template, dilutions 1:10, 1:20, and 1:50 were used. Those PCR products that gave brighter and cleaner signals after submitted to gel electrophoresis were selected for continuing the cloning and sequencing process.

Once this procedure was complete, the retrieved sequences were submitted to BLAST Tool (NCBI), and relative species of bacteria were found. The main feature that could be pointed out from the results was the decrease of diversity with the increase of conductivity of the influent. It suggests that osmotic pressure selects the most resistant species and statins to keep developing and growing. However, regarding to DOC metabolizing, it does not seem to hinder the performance of the bioreactor, what suggests that different structure consortiums, due to characteristics of the medium, could be developing similar functions.

Regarding to the number to uncultured bacteria, which are the majority of the species in every sample, indicate how difficult is for culture dependent media to deeply characterize this complicate biosystems, and how relevant are molecular biology techniques to solve this issue.

Proteobacteria domain was the most abundant domain in every case (only uncultured bacteria outnumbered this domain for B2 load). The relationship between the members of this domain can be seen in the phylogenetic trees depicted in fig. 52, and 53. They were drawn by MegaAlign Tool (LaserGen, DNASTAR), after align the sequences by the Clustal V Method (Higgins 1994).

The length of each pair of branches represents the distance between sequence pairs, while the units at the bottom of the tree indicate the number of substitution events that differentiate one sequence from another. The fact that for column stages 2 and 3, the maximum substitution events is so low, indicating a close similarity between sequences, corroborates the decreasing diversity of those samples.

According to Wagner and Loy (Wagner and Loy 2002), *Beta-*, *Alpha-* and *Gammaproteobacteria* are frequently retrieved in wastewater treatment plants, especially *Betaproteobacteria* that play important roles degrading a variety of pollutants. *Rhodocyclales* and *Burkholderiales* were specially abundant. While the first have been identified as bioremediators of anthropogenic biotechnological systems (Loy et al. 2005), there is an especially interesting case among *Rhodocyclales*. Certain strain of *Comamonas* was revealed as capable of degrading certain organochlorine herbicides (Müller et al. 1999), although no bidegradation of the pesticides themselves was observed.

Regarding to *Gammaproteobacteria*, they are known to exist normally in aerobic biosystems as the main bacterial groups (Lee et al. 2003; Wong et al. 2005; Xia et al. 2010) and in DOC degrading in nutrient-rich environment (Poretsky et al. 2010), even in sea-salinity media (Manes et al. 2011). Among them *Pseudomonas* presents a strain identified as nicotine degrader in tobacco wastes by (Zhong et al. 2010). This suggests this kind of bacteria could also perform neonicotinoid pesticide degradation as imidacloprid, with structures derived from the alkaloid's, if the optimal conditions of feed and aeration could be found.

Numerous *Bacteroidetes* were also found in B1 and B2. Together with *Proteobacteria*, these phylums are known to be the most prominent heterotrophic organisms in marine surface waters (Stevens et al. 2005) and exist normally in aerobic biosystems (Deng et al. 2012), what fits the environment of the column. *Bacteroidetes* are also found as dominant phylum in 16s rRNA libraries from agricultural soil samples (Jangid et al. 2008; Janssen 2006), especially *Sphingobacteria* class, which are common in both named stages, *Chitinophagaceae* and *Saprospiraceae* in stage 2, and *Terrimonas* in stage 1. The relationship of this phylum with agricultural earth could indicate its resistance to pesticide products. Furthermore, Deng and colleagues (Deng et al. 2012)

stated that this phylum is involved in the degradation of a variety of pollutants, and play important roles in wastewater treatment.

Several microbiological testimonies of nitrification and denitrification were present in all stages of the column, although chemical proves could not be found. This could indicate that the particular process was taking place but in such a small proportion that it could not be detected analytically. This could be due to the high quantities of nitrates, in the shape of KNO_3 , present in the media that could be masking subtle changes in nitrogen content.

Figure 12. Proteobacteria phylogenetic tree for column at stage 1.

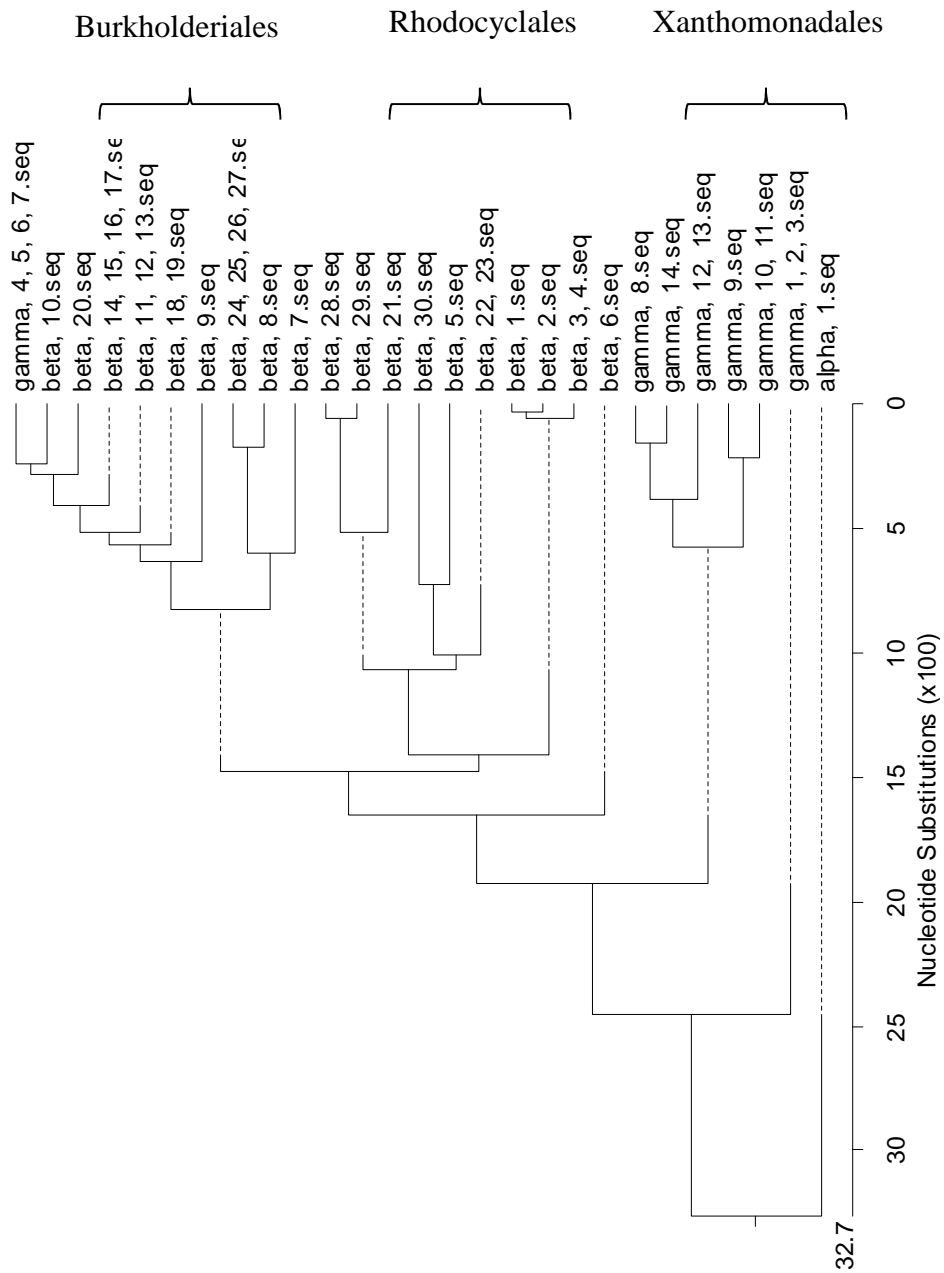
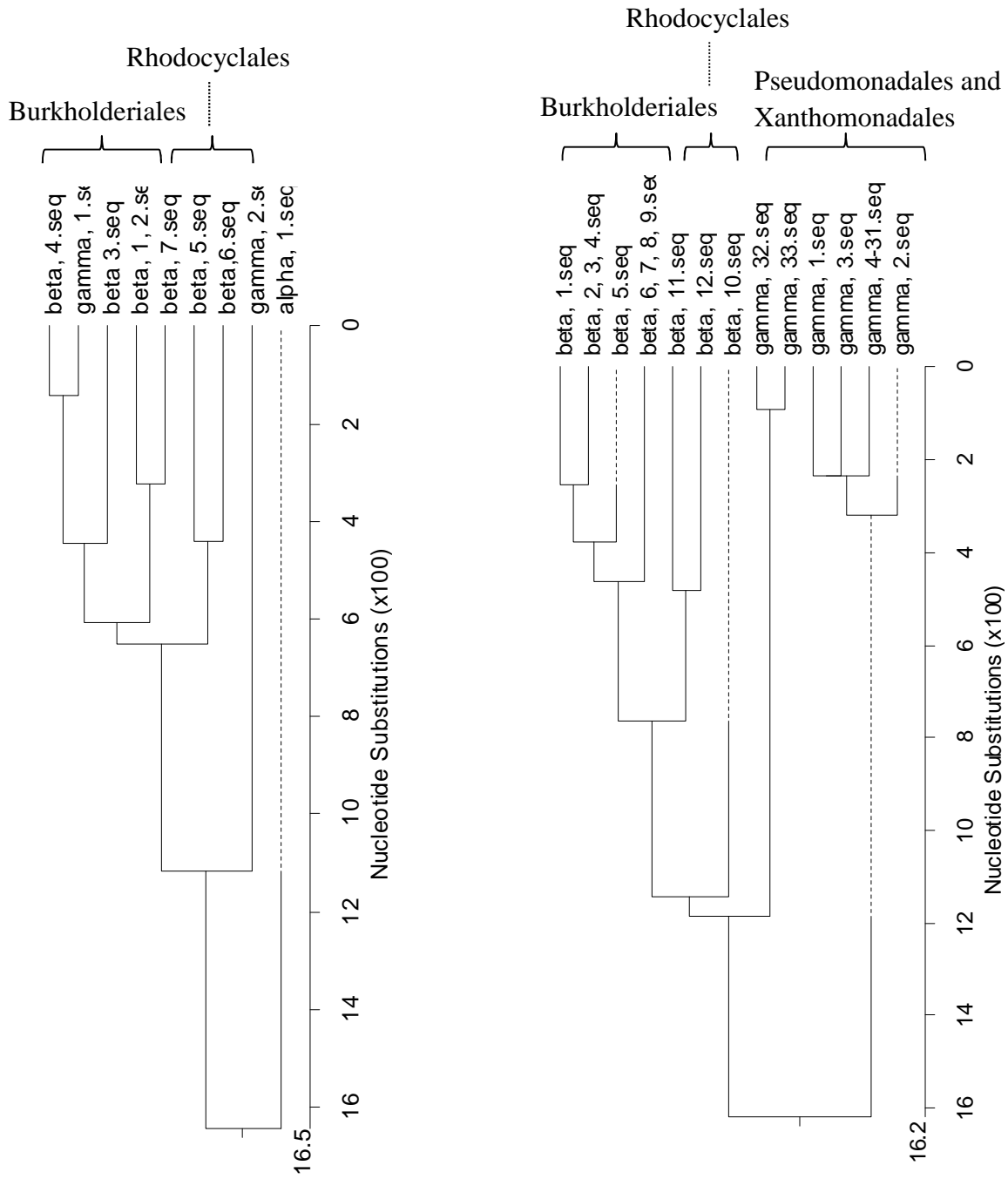


Figure 13. Proteobacteria phylogenetic tree for column at stages, 2 (left) and 3 (right).



5

CONCLUSIONS

The main and most important conclusion that could be retrieved from this work is that the coupling between photo-Fenton reaction and slow sand filtration column could be an effective treatment alternative for implementing the recycling strategies of hydroponics greenhouse leachates proposed by CENIT-MEDIODIA Project. Even in the case of the highest salinity conditions, the integrated system seemed to be promising due to the optimal results obtained for the biocompatibility essay of photo-Fenton pretreated effluents with salinities between 11 to 50 mS·cm⁻¹.

Regarding to photo-Fenton reaction, it could have been seen how it is able to efficiently degrade pesticides load, despite the existence of interferences such as endogenous catalyst inhibition and salinity influences. This possible conditioning of the reaction has to be taken into account in order to optimize reagent concentration and other working conditions, given that they can either interfere positively or negatively, depending to the objectives of the process.

It could be also concluded that good results obtained indicate that solar photo-Fenton could be a good alternative to the artificially irradiated process. It would have many advantages on its in-field implementation, given the availability of sun radiation in the surroundings of greenhouse premises, what improves noticeably the economical aspect.

Focusing on the bioreactor performance, it has been seen how starting from inoculums completely aliens to hydroponics leachates, the pesticides, the by-products, the salinity, etc., biosystems have been able to overcome the shock and bloom in these media, mineralizing their biodegradable content (increased by photo-Fenton pretreatment). The reactors were no able to biodegrade target compounds by themselves, though, but the presence of the xenobiotics did not inhibit biomass development, neither did to DOC consumption.

An especially interesting conclusion could be retrieved from the use of MBTs. Although salinity seemed not to dramatically hinder the performance of the slow sand filtration reactor regarding to DOC degradation, diversity o biomass decreased noticeably. This states how different could be microbial consortiums developing the same tasks due to certain changes in the medium.

The high amount of retrieved sequences related by BLAST with uncultured microorganisms, and the descriptive level of the microbial community that can be obtained by these technologies makes them a promising tool to improve the knowledge of the bacterial populations and their functions in reactors performance, in comparison to culturable dependant technologies.